THE COLLISIONAL BEHAVIOUR OF GROUND STATE BISMUTH ATOMS, Bi($6^4S^0_{3/2}$), WITH ALKYL BROMIDES STUDIED BY TIME-RESOLVED ATOMIC RESONANCE FLUORESCENCE AT λ = 306.77 nm (Bi($7^4P_{1/2}$)–Bi($6^4S^0_{3/2}$)) FOLLOWING PULSED IRRADIATION: KINETICS, RADIATION TRAPPING AND FLUORESCENCE QUENCHING OF Bi($7^4P_{1/2}$)

CHARLES F. BELL and DAVID HUSAIN

Department of Physical Chemistry, The University of Cambridge, Lensfield Road, Cambridge CB2 1EP (Gt. Britain)

(Received January 31, 1984; in revised form March 13, 1984)

Summary

The kinetic study of ground state bismuth atoms, Bi($6^4S^0_{3/2}$), has been investigated by time-resolved atomic resonance fluorescence at λ = 306.77 nm (Bi($7^4P_{1/2}$)–Bi($6^4S^0_{3/2}$)) in the "single-shot" mode following pulsed irradiation. Bi($6^4S^0_{3/2}$) was generated by the flash photolysis of $Bi(CH_3)_3$ in the presence of excess helium buffer gas and monitored as a function of time with various added bromine-containing molecules as reactants. Absolute second-order rate constants k_{RBr} (cm^3 $molecule^{-1}$ s^{-1}) (T = 300 K; errors, 2σ) are reported for the removal of Bi($6^4S^0_{3/2}$) by the following molecules: Br_2, $(5.3 \pm 1.8) \times 10^{-13}$; CH_2Br_2, $(9.0 \pm 1.3) \times 10^{-15}$; CH_3Br, $(1.8 \pm 0.4) \times 10^{-15}$; C_2H_5Br, $(4.1 \pm 0.7) \times 10^{-15}$; n-C_3H_7Br, $(1.2 \pm 0.1) \times 10^{-14}$. These results are compared with analogous rate data for the reaction of ground state lead atoms, Pb(6^3P_0). We also present detailed calculations of radiation trapping using various models including the diffusion theory of radiation involving a characteristic mean free path of an emitted photon and a more generalized transport theory for the (Bi($7^4P_{1/2}$)–Bi($6^4S^0_{3/2}$)) transition, including the effect of nuclear hyperfine interaction. Consideration is given in the present paper to radiation trapping calculations for atomic densities where the simplifying approximations resulting from the use of "low equivalent opacities" break down. The results of these calculations are presented for various models which lead to relations describing the variation in the effective mean radiative lifetime with atomic density and the functional relationship between fluorescence intensity and particle density.

1. Introduction

We have recently described an experimental arrangement for the kinetic study of ground state atomic bismuth, Bi($6^4S^0_{3/2}$), generated by pulsed

0047-2670/84/$3.00

irradiation and monitored by time-resolved atomic resonance fluorescence at $\lambda = 306.77$ nm ($Bi(7^4P_{1/2})$–$Bi(6^4S^0_{3/2})$) [1]. This was employed for various kinetic measurements including the rates of the third-order reactions between Bi + C_2H_2 + He, Bi + O_2 + M and Bi + NO + M (M ≡ He, N_2 and CF_4), that of the second-order reaction between Bi and N_2O and of the fluorescence quenching cross sections of $Bi(7^4P_{1/2})$ by the molecules employed in the kinetic measurements [1, 2]. These investigations followed earlier developments of this time-resolved technique when applied to $Bi(6^4S^0_{3/2})$ [3]. The technique has also been modified in various forms for kinetic studies of the ground states of the other group V elements, $Sb(5^4S^0_{3/2})$ [4], $As(4^4S^0_{3/2})$ [5], $P(3^4S^0_{3/2})$ [6] and $N(2^4S^0_{3/2})$ [7, 8]. Connor *et al.* [9] have reported fluorescence quenching cross sections using integrated plate intensity measurements following the flash photolysis of bismuth trimethyl, $Bi(CH_3)_3$. However, to the best of our knowledge, the above time-resolved resonance fluorescence measurements and that reported by Husain and Slater [10] using resonance absorption for the kinetic study of Bi + C_2H_2, C_2H_4 + M and reaction with NO, O_2 and N_2O constitute the summary of absolute rate measurements for ground state bismuth atoms.

In this paper we describe a kinetic study of the collisional removal of $Bi(6^4S^0_{3/2})$ with the molecules Br_2, CH_3Br, CH_2Br_2, C_2H_5Br and n-C_3H_7Br using time-resolved atomic resonance fluorescence following pulsed irradiation. Absolute second-order rate constants are reported for the reactions and these are compared, where possible, with analogous rate data for the heavy group IV element, $Pb(6^3P_0)$, obtained by time-resolved resonance absorption measurements [11]. We also present detailed calculations on radiation trapping [12] for the transition at $\lambda = 306.77$ nm using various models including those pertinent to high atomic densities. The results of such calculations are used to estimate an effective mean radiative lifetime for the resonance transition in order to correct previous measurements that we have reported for collision cross sections describing fluorescence quenching of $Bi(7^4P_{1/2})$ [1, 2] which were based on the use of the natural radiative lifetime ($\tau_e = 5.9$ ns) [13] in the Stern–Volmer analyses.

2. Experimental details

The experimental arrangement for the kinetic study of $Bi(6^4S^0_{3/2})$, generated by pulsed irradiation of low pressures of $Bi(CH_3)_3$ in the presence of excess helium buffer gas and monitored by time-resolved resonance fluorescence in the "single-shot" mode at $\lambda = 306.77$ nm ($Bi(7^4P_{1/2})$–$Bi(6^4S^0_{3/2})$, $\tau_e = 5.9$ ns [13]), was essentially that described in detail previously [1, 2] with some modification to the flash-lamp photolysis source. The flash-lamp was shortened by removing the metallic cylinder comprising the buffer volume between the pulsed discharge region and the Pyrex tubing for physical coupling to the metallic reaction vessel, with optical coupling via an LiF window. The reaction vessel itself, with the Cassegrain mirror for greater

light gathering power of the fluorescence signals, was unchanged. This closer optical coupling permitted concentrations of $Bi(CH_3)_3$ at least one-tenth of those used hitherto [1, 2] to generate atomic densities of $Bi(6^4S^0_{3/2})$ sufficiently high for time-resolved atomic resonance fluorescence in the single-shot mode. Following the pulsed generation of $Bi(6^4S^0_{3/2})$, the ground state bismuth atoms were optically excited to the $Bi(7^4P_{1/2})$ state by means of the high intensity microwave-powered source (75 W; microwave generator, EMS Mircotron 200 mark 2; 2450 MHz) adapted [1] to the design of Beenakker and Boumans [14 - 16] operating in the TM_{010} mode and employing sublimed BiI_3 in a sealed quartz capsule as the source of the atomic resonance transition. The orthogonal arrangement for the flash-lamp, the spectroscopic source and the photoelectric detection system (EMI photomultiplier tube 9635QB; voltage, about 750 V) has been described previously. The resonance fluorescence signal was optically isolated with an interference filter (Oriel Corporation, U.S.A.; type 521-3130; transmission at λ = 306.77 nm, about 8%). The resulting photoelectric signals representing the decay of resonance fluorescence were amplified without distortion [17], captured and stored in digital form in a transient recorder (Data Laboratories DL 905) and punched onto paper tape in ASCII code (Datadynamics punch 1133) for subsequent analysis in the University of Cambridge IBM 3081 computer. With the exception of n-C_3H_7Br (AnalaR), which was subjected to several freeze–pump–thaw cycles at liquid nitrogen temperature and finally fractionally distilled to this temperature, all materials ($Bi(CH_3)_3$, BiI_3, He, Kr (for the flash-lamp), Br_2, CH_3Br, CH_2Br_2 and C_2H_5Br) were essentially prepared as described in previous publications [1, 2, 11].

3. Results and discussion

3.1. Photolysis of $Bi(CH_3)_3$ and alkyl bromides RBr

As we indicated in previous papers [1, 2] the degree of photolysis of $Bi(CH_3)_3$ can be estimated, in principle, by the integrated attenuation of actinic radiation from the flash-lamp by $Bi(CH_3)_3$:

$$I_{abs} = \int I_\lambda \exp\{-\epsilon(\lambda)cl'\}[1 - \exp\{-\epsilon(\lambda)cl\}]\, d\lambda \qquad (1)$$

where l' is the path length from the LiF window of the flash-lamp to the face of the (unit) reaction cell and l is the (unit) path length of the reaction cell. The reaction cell is that volume within the reaction vessel which is formed by the overlap of the solid angles of light from the flash-lamp and resonance source and the geometrical coupling to the detector including the effect of the Cassegrain mirror. If the light output of the flash-lamp can be approximated as a black body radiator at a temperature of 6500 °C [18] then the standard Planck distribution, $U(\lambda, T)$, may by substituted for I_λ in eqn. (1):

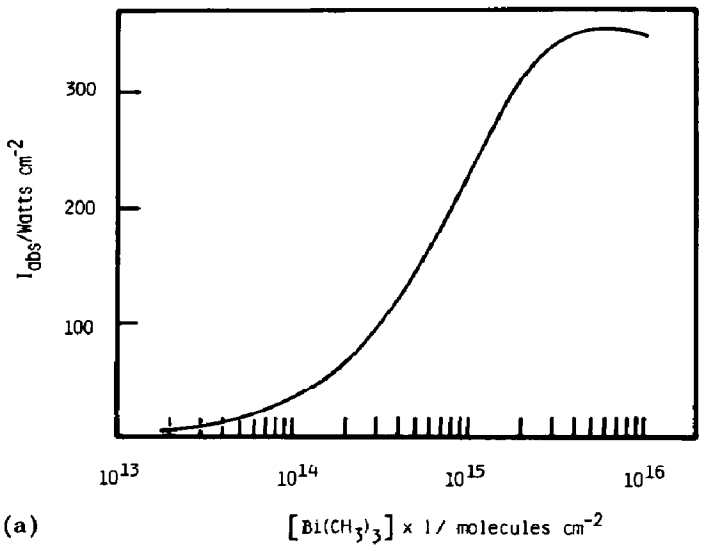

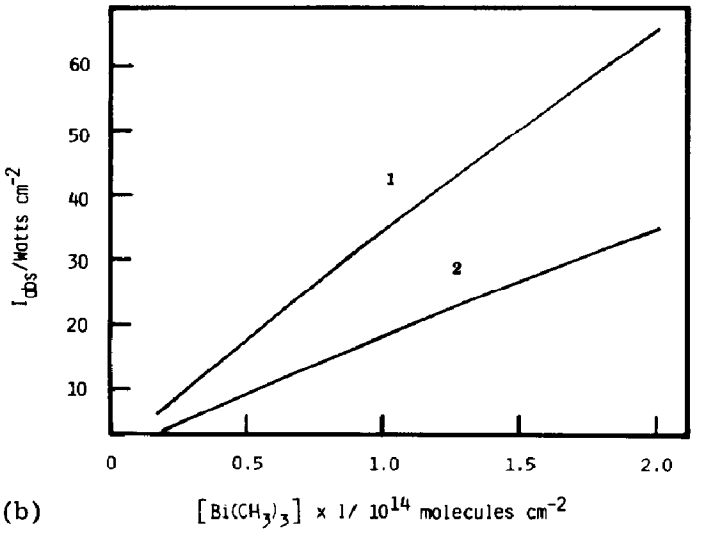

Fig. 1. Attenuation of the calculated black body output for $T = 6500$ °C from the flash photolysis lamp by the UV spectrum of $Bi(CH_3)_3$: (a) $[Bi(CH_3)_3] \times l = 10^{13} - 10^{16}$ molecules cm^{-2}; (b) $[Bi(CH_3)_3] \times l = (0 - 2) \times 10^{14}$ molecules cm^{-2} (curve 1, present flash photolysis lamp; curve 2, flash photolysis lamp following ref. 1).

$$U(\lambda, T = 6773\ \mathrm{K}) = \Omega \frac{2\pi c^2 h}{\lambda^5} \Big/ \left\{ \exp\left(\frac{hc}{\lambda k T}\right) - 1 \right\} \tag{2}$$

where Ω is a term to account for the area of incident radiation. In addition, from UV absorption measurements of $Bi(CH_3)_3$, $\epsilon(\lambda)$ (ϵ_{max}(base e) = 1.2×10^5 M^{-1} cm^{-1}) may be approximated by

$$\epsilon(\lambda) = \epsilon_{max} \exp\{c(\lambda \pm \lambda_{max})\} \tag{3}$$

from $\lambda = 145$ nm to $\lambda = 270$ nm ($\lambda_{max} = 208$ nm). Figure 1(a) shows the result of such a calculation for the present flash-lamp and reaction vessel

($l' = 6$ cm). Figure 1(b) shows that I_{abs} per unit area of the reaction cell *versus* $[Bi(CH_3)_3] \times l$ over the range of $[Bi(CH_3)_3]$ used in this and previous studies is virtually linear; thus, we may expect that the rate of destruction of $Bi(CH_3)_3$ is directly proportional to the concentration of $Bi(CH_3)_3$ added. The slope of Fig. 1(b), curve 1, is 1.9 MeV s^{-1} and that of Fig. 1(b), curve 2, is 1.0 MeV s^{-1}. Hence

$$[Bi(6^4S^0_{3/2})] \text{ (atoms cm}^{-3}) \leqslant \tau_{FL}\Phi \times \text{slope} \times \frac{[Bi(CH_3)_3]}{D} \quad (4)$$

where D is the minimum energy necessary to decompose $Bi(CH_3)_3$ completely to produce ground state bismuth atoms, τ_{FL} is the duration of the actinic irradiation and Φ is the quantum yield. Substitution of "reasonable" values for the parameters in eqn. (4) ($D^0(Bi{-}CH_3) = 1.48$ eV [19]) yields concentrations of $Bi(6^4S^0_{3/2})$ which are high (see later).

The apparent second-order rate constant for the removal of $Bi(6^4S^0_{3/2})$ by $Bi(CH_3)_3$ itself, namely that derived from the slope of the first-order coefficient k' for the decay of $Bi(6^4S^0_{3/2})$ (see later), *versus* $[Bi(CH_3)_3]_{initial}$ yields a value of $k_2 = (3.0 \pm 0.2) \times 10^{-13}$ cm^3 molecule^{-1} s^{-1} ($T = 300$ K; error, 2σ). This value is sensibly invariant with $[Bi(CH_3)_3]_{initial}$ (Fig. 2). This may be compared with that for $k(Sb(5^4S^0_{3/2}) + Sb(CH_3)_3)$ derived from time-resolved resonance absorption measurements to yield $(2.3 \pm 0.2) \times 10^{-11}$ cm^3 molecule^{-1} s^{-1} (300 K; error, 1σ) [20]. If, in fact, the apparent second-order rate constant for $Bi(6^4S^0_{3/2}) + Bi(CH_3)_3$ reflected the magnitude of the concentration of the photochemical precursor remaining after irradiation and the true rate constant were similar to that for $Sb(5^4S^0_{3/2}) + Sb(CH_3)_3$, the comparison would imply a decomposition to $Bi(CH_3)_2$, $BiCH_3$ and

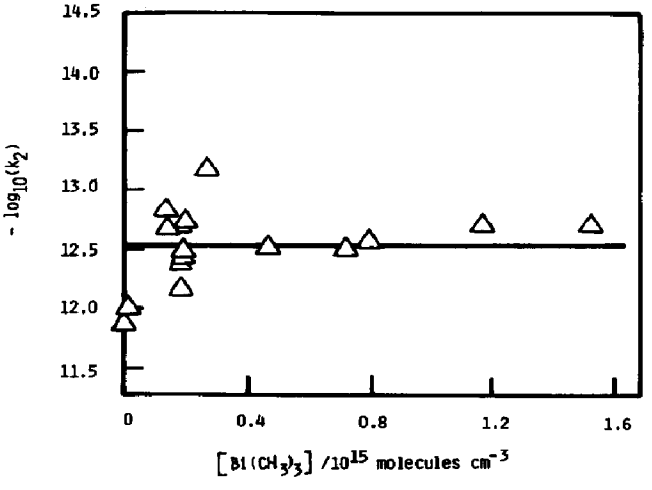

Fig. 2. Variation in the second-order rate constant k_2 for the collisional removal of $Bi(6^4S_{3/2})$ as a function of the concentration of $Bi(CH_3)_3$ obtained by time-resolved atomic resonance fluorescence at $\lambda = 306.8$ nm ($Bi(7^4P_{1/2}) \rightarrow Bi(6^4S_{3/2})$) following pulsed irradiation.

$Bi(6^4S^0_{3/2})$ of about 99%. It will be shown later that the majority of these photolysis fragments appear to be the first two species, rather than the desired free ground state bismuth atom.

Alkyl bromides and bromine molecules also absorb in the near-UV region [21, 22] but more weakly than $Bi(CH_3)_3$ ($\epsilon_{max}(Bi(CH_3)_3)/\epsilon_{max}(CH_3Br) = 230$ and $\epsilon_{max}(Bi(CH_3)_3)/\epsilon_{max}(Br_2) = 310$). Calculations using eqns. (1) - (4) for $RBr \equiv CH_3Br$ show that given the present geometrical arrangement and unit reaction cell with CH_3Br alone

$$[Br] = [CH_3] \leqslant (2.7 \text{ keV s}^{-1})\,[CH_3Br] \times \frac{\tau_{FL}\Phi}{D^0(CH_3\text{—}Br)}$$

assuming that CH_3—Br is the only bond undergoing photodissociation [23, 24] and $[CH_3Br] < 1 \times 10^{17}$ molecules cm^{-3}. For $D^0(CH_3\text{—}Br) = 2.97$ eV [25] and $\tau_{FL}\Phi = 3\ \mu s$, the degree of photolysis is less than 0.3%.

The preceding discussion indicates that in *experimental* terms the method used for this study relies on some measure of filtration of the actinic radiation to prevent photolysis of RBr. In resonance absorption measurements on the rate processes undergone by $Pb(6^3P_0)$, this was provided for by means of a double-walled reaction vessel containing the alkyl bromide itself [11]. In addition to the unwanted destruction of RBr, however, there are two other sources of systematic experimental error: (1) reaction of RBr with the precursor itself and (2) a screening effect by absorption of light from the flash-lamp by RBr leading to a lower production of ground state bismuth atoms from $Bi(CH_3)_3$.

3.2. Kinetics of $Bi(6^4S^0_{3/2})$

The improvement in the optical coupling between the source of actinic radiation and the reactor resulting from the modification to the flash-lamp (see Section 2) can clearly be seen in Fig. 3(a) which gives an example of the time variation of the resonance fluorescence signal (I_F *versus* t) at $\lambda = 306.77$ nm ($Bi(7^4P_{1/2})$–$Bi(6^4S^0_{3/2})$) indicating the decay of ground state bismuth atoms generated by the pulsed irradiation of $Bi(CH_3)_3$ at a concentration considerably lower than that employed in earlier investigations [1, 2]. Figure 3(b) gives an example of an analogous plot illustrating the greater decay rate for $Bi(6^4S^0_{3/2})$ with the addition of C_2H_5Br. We have demonstrated hitherto [1 - 3] that the time-dependent resonance fluorescence signal is given by the form

$$I_F(t) = \frac{\phi[Bi(6^4S^0_{3/2})]_{t=0} \exp(-k't)}{1 + k_Q[Q]/gk_f} \qquad (5)$$

where k' is the overall first-order coefficient for the decay of $Bi(6^4S^0_{3/2})$ and is the primary object of kinetic interest. k_Q is the absolute second-order rate constant for the fluorescence quenching of $Bi(7^4P_{1/2})$ by the gas Q and is also of interest in this paper. The term gk_f is the effective fluorescence decay rate with no quenching gas present. Without radiation trapping $gk_f = 1/\tau_e$ and with radiation trapping $gk_f < 1/\tau_e$. Account is taken of the steady light

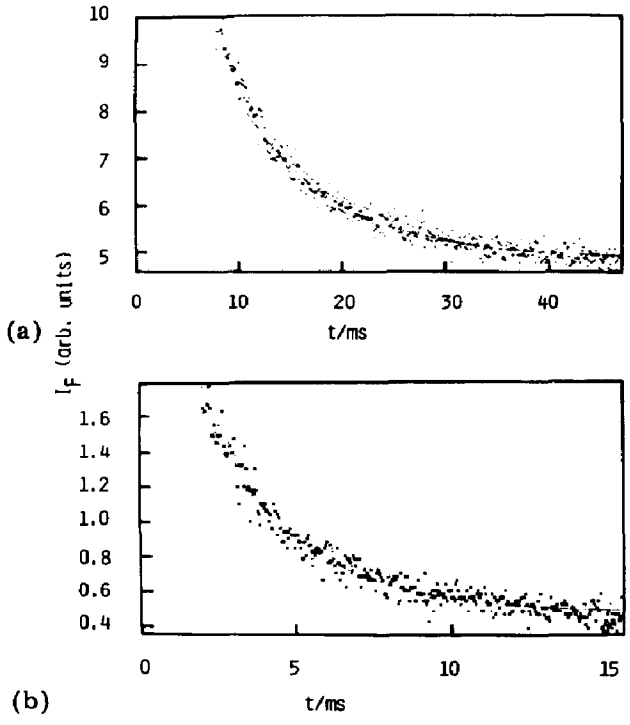

Fig. 3. Digitized time variation in the light intensity I_F at λ = 306.8 nm ($Bi(7^4P_{1/2}) \rightarrow Bi(6^4S_{3/2})$) indicating the decay of resonance fluorescence due to ground state bismuth atoms for (a) $[C_2H_5Br] = 0$ and (b) $[C_2H_5Br] = 1.1 \times 10^{17}$ molecules cm^{-3} ($[Bi(CH_3)_3] = 1.9 \times 10^{14}$ molecules cm^{-3}; $[He] = 6.9 \times 10^{17}$ atoms cm^{-3}; E = 320 J): ×, data points; ——, computerized curve fitting to the form $I_F = \theta_1 + \theta_2 \exp(-k't)$.

signal at λ = 306.77 nm from the resonance source as seen from inspection of Fig. 3, where $I_F(t)$ clearly approaches a finite value at infinite time. Hence, I_F is employed in the form

$$I_F = \theta_1 + \theta_2 \exp(-k't) \tag{6}$$

which is fitted to the digitized data points [1, 26]. The full curves in Fig. 3 indicate the resulting fit by computer of the data to the form of eqn. (6) and Fig. 4 shows the analogous first-order kinetic plots ($\ln(I_F - \theta_1)$ *versus* t) for the data shown in Fig. 3. Figure 5 shows examples of fitting by computer of the digitized output of the atomic decays to the form ($I_F - \theta_1$) *versus* t for different concentrations of C_2H_5Br (Fig. 5(a)) and Br_2 (Fig. 5(b)).

The values of k' resulting from the data analyses can be expressed in the form

$$k' = K' + \frac{\beta}{p_{He}} + (1 - \delta)k'_{RBr}[RBr] \tag{7}$$

where δ represents the fraction of RBr removed (by photolysis and reaction with $Bi(CH_3)_3$) before the reaction Bi + RBr → BiBr + R takes place. Thus, it is necessary to carry out these experiments with lower pressures of RBr

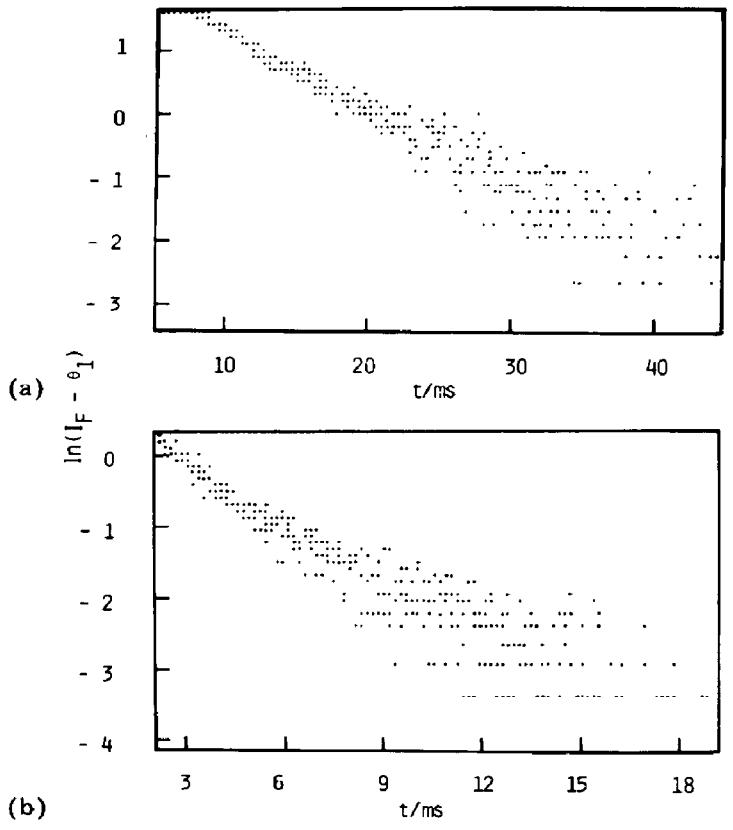

Fig. 4. Computerized output of the digitized first-order kinetic plots derived from time-resolved atomic resonance fluorescence measurements at $\lambda = 306.8$ nm ($Bi(7^4P_{1/2}) \rightarrow Bi(6^4S_{3/2})$) due to the kinetic removal of ground state bismuth atoms for (a) $[C_2H_5Br] = 0$ and (b) $[C_2H_5Br] = 1.1 \times 10^{17}$ molecules cm^{-3} ($[Bi(CH_3)_3] = 1.9 \times 10^{14}$ molecules cm^{-3}; $[He] = 6.9 \times 10^{17}$ atoms cm^{-3}; $E = 320$ J): ●, data points; ——, computerized fitting to the form $\ln(I_F - \theta_1)$ *vs.* t.

($\delta \rightarrow 0$ as $[RBr] \rightarrow 0$) than the expected rate constant [11] would ideally demand. (Nevertheless, $[RBr] \gg [Bi(6^4S^0_{3/2})]$.) The term β/p_{He} in eqn. (7) represents the first-order decay coefficient for the loss of $Bi(6^4S^0_{3/2})$ by diffusion [27]. K' principally represents first-order loss of $Bi(6^4S^0_{3/2})$ by $Bi(CH_3)_3$. The role of diffusion at different total pressures with helium buffer gas can be seen in Fig. 6 which is a plot of k' *versus* $1/p_{He}$, in accord with eqn. (7), for the decay of $Bi(6^4S^0_{3/2})$ in the presence of Br_2. It is important to note here that although it might be expected that increasing [He] would increase the number of recombined bromine molecules within 50 ms after photolysis and thus cause a (non-linear) trend downwards of k' *versus* $1/p_{He}$ (eqn. (7)), no such trend was observed at low $[Br_2]$ (Fig. 6). For measurements of k' at a fixed total pressure, eqn. (7) can be written as

$$k' = K + k_{RBr}[RBr] \qquad (8)$$

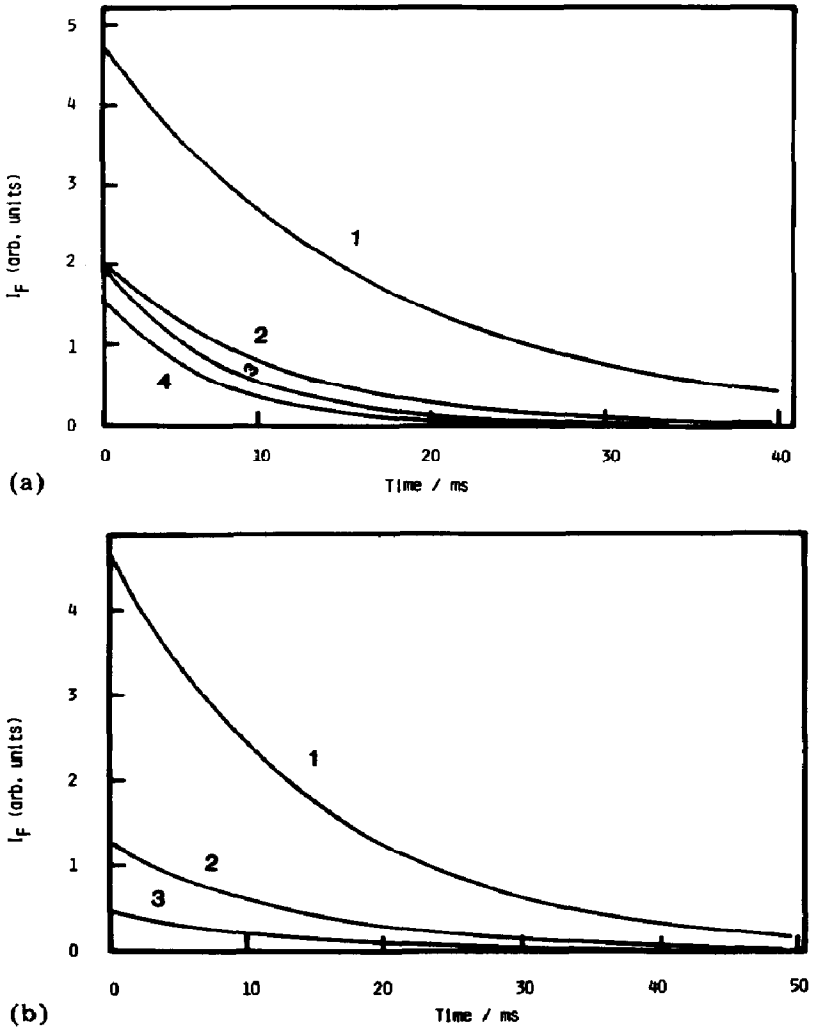

Fig. 5. Computerized curve fitting of the experimental intensity profiles for the decay of $Bi(6^4S_{3/2})$ obtained by time-resolved atomic resonance fluorescence at $\lambda = 306.8$ nm ($Bi(7^4P_{1/2}) \rightarrow Bi(6^4S_{3/2})$) (($I_F - \theta_1$) *vs.* t) in the presence of C_2H_5Br and Br_2 ($E = 320$ J): (a) C_2H_5Br ($[Bi(CH_3)_3] = 1.0 \times 10^{13}$ molecules cm^{-3}; $[He] = 3.2 \times 10^{17}$ atoms cm^{-3}) (curve 1, $[C_2H_5Br] = 0$; curve 2, $[C_2H_5Br] = 4.6 \times 10^{15}$ molecules cm^{-3}; curve 3, $[C_2H_5Br] = 8.0 \times 10^{15}$ molecules cm^{-3}; curve 4, $[C_2H_5Br] = 9.0 \times 10^{15}$ molecules cm^{-3}); (b) Br_2 ($[Bi(CH_3)_3] = 2.9 \times 10^{13}$ molecules cm^{-3}; $[He] = 7.2 \times 10^{17}$ atoms cm^{-3}) (curve 1, $[Br_2] = 1.9 \times 10^{14}$ molecules cm^{-3}; curve 2, $[Br_2] = 2.6 \times 10^{14}$ molecules cm^{-3}; curve 3, $[Br_2] = 3.5 \times 10^{14}$ molecules cm^{-3}).

and hence k_{RBr} can be derived from the slope of $(k' - K)$ *versus* [RBr], K having been determined in the absence of RBr.

Figure 7 shows the variation in the first-order decay coefficient k' for the removal of $Bi(6^4S^0_{3/2})$ relative to the term K for removal in the absence of RBr (eqn. (8)), with $[CH_3Br]$, $[C_2H_5Br]$ and $[n\text{-}C_3H_7Br]$. The decay of $Bi(6^4S^0_{3/2})$ in the presence of CH_2Br_2 as in the presence of Br_2 demonstrated kinetic behaviour similar to that reported for $Pb(6^3P_0)$ in the presence of

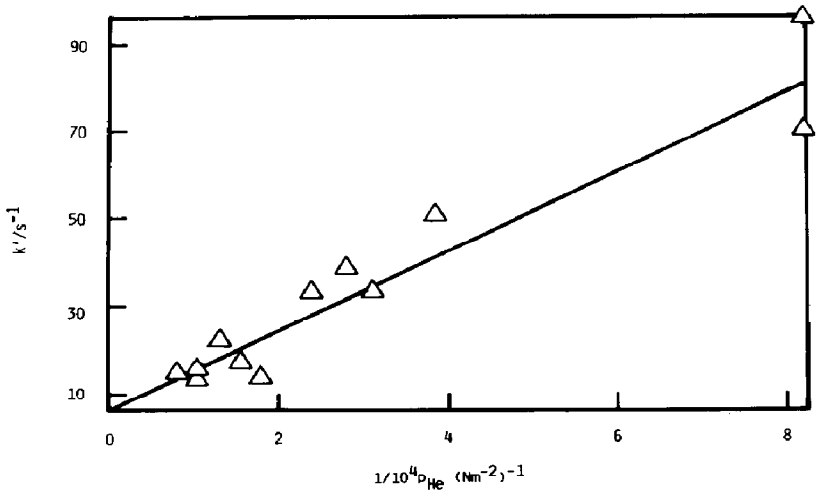

Fig. 6. Variation in the pseudo-first-order rate coefficient k' for the decay of $Bi(6^4S_{3/2})$ in the presence of Br_2 and He (k' *vs.* $1/p_{He}$) indicating the effects of diffusion and second-order kinetics ($[Bi(CH_3)_3] = 2.3 \times 10^{13}$ molecules cm^{-3}; $[Br_2] = 9.3 \times 10^{13}$ molecules cm^{-3}; $E = 320$ J).

CH_3CHBr_2 [11]. Thus, the variation in k' with $[CH_2Br_2]$ and $[Br_2]$ showed strong curvature at high concentrations of CH_2Br_2 and Br_2 (Figs. 8 and 9), presumably reflecting the effect of complex kinetics with a back reaction regenerating ground state atomic bismuth. We employ here the empirical procedure of Cross and Husain [11] by using the equation

$$k' - K = \frac{\alpha[RBr]}{1 + \gamma[RBr]} \tag{9}$$

rather than taking the initial slope. Equation (9) uses all the data when plotted in the form $[RBr]/(k' - K)$ *versus* $[RBr]$ to yield $1/\alpha$ from the intercepts, as shown in Figs. 8(b) and 9(b) for CH_2Br_2 and Br_2 respectively. The present measurements with Br_2 may be contrasted with those attempted for the analogous process for $Pb(6^3P_0)$ where reaction between the photochemical precursor, $Pb(C_2H_5)_4$, and Br_2 prevented any measurement of the absolute rate constant. The absolute second-order rate constants for the reaction of $Bi(6^4S^0_{3/2})$ with the alkyl bromides and Br_2 are presented in Table 1 together with analogous data for $Pb(6^3P_0)$.

The thermochemistry of bromine atom abstraction for the various reactions investigated here naturally rests on the bond dissociation energy of Bi—Br for which we take the value of $D^0(Bi—Br) = 2.74 \pm 0.01$ eV following Gaydon [28]. This is based on Gaydon's conclusion that a linear Birge–Sponer extrapolation of the $A(0^+)$–$X(0^+)$ system of BiBr yields dissociation products correlating with $Br(4^2P_{3/2})$ rather than with $Br(4^2P_{1/2})$ [29, 30] which would yield a lower value of $D^0(Bi—Br) = 2.28$ eV. Huber and Herzberg [31] do not quote a value for $D^0(Bi—Br)$. The contrast with $D^0(Pb—Br) = 2.5 \pm 0.4$ eV [32, 33] is noteworthy in the present context involving the comparison of rate data for bromine atom abstraction by

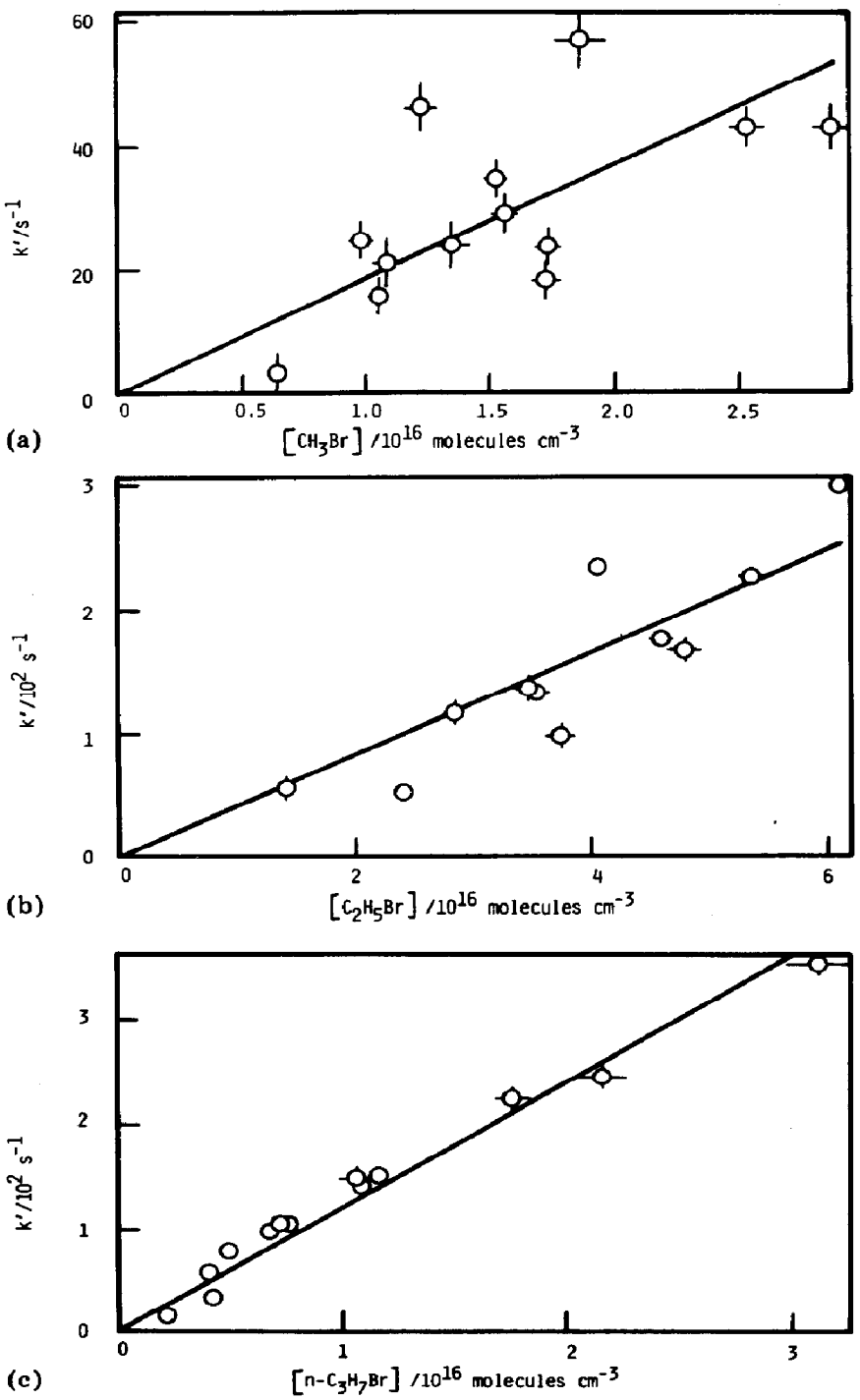

Fig. 7. Variation in the pseudo-first-order rate coefficient k' (diffusion corrected and normalized) for the decay of Bi($6^4S_{3/2}$) in the presence of (a) CH_3Br, (b) C_2H_5Br and (c) n-C_3H_7Br (E = 320 J): (a) CH_3Br ([Bi$(CH_3)_3$] = 3.6 × 10^{13} molecules cm^{-3}; [He] = 3.6 × 10^{17} atoms cm^{-3}); (b) C_2H_5Br ([Bi$(CH_3)_3$] = 4.8 × 10^{13} molecules cm^{-3}; [He] ≈ 10 × 10^{17} atoms cm^{-3}); (c) n-C_3H_7Br ([Bi$(CH_3)_3$] = 1.2 × 10^{13} molecules cm^{-3}; [He] = 3.1 × 10^{17} atoms cm^{-3}).

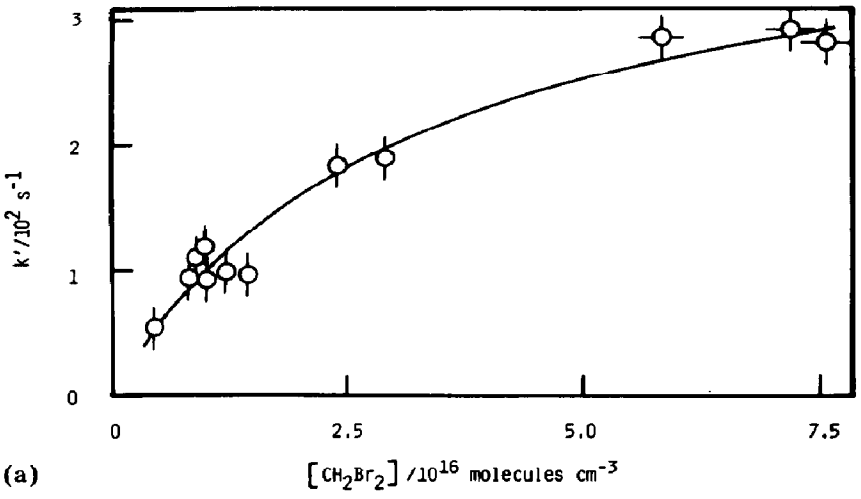

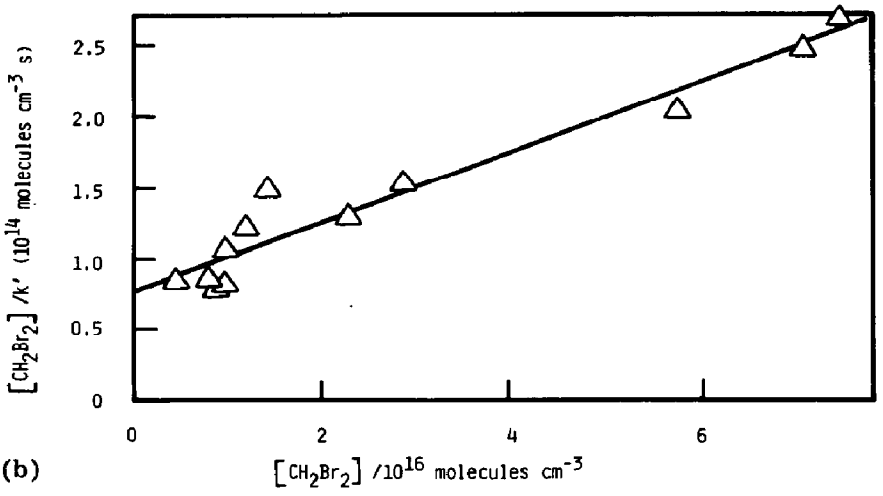

Fig. 8. Variation in the pseudo-first-order rate coefficient k' (diffusion corrected and normalized) for the decay of $Bi(6^4S_{3/2})$ in the presence of CH_2Br_2 ($[Bi(CH_3)_3] = 1.6 \times 10^{13}$ molecules cm^{-3}; $[He] = 5.3 \times 10^{17}$ atoms cm^{-3}; $E = 320$ J): (a) k' *vs.* $[CH_2Br_2]$; $[CH_2Br_2]/k'$ *vs.* $[CH_2Br_2]$.

$Bi(6^4S^0_{3/2})$ and $Pb(6^3P_0)$ (Table 1) as the thermochemistry for a number of such processes is close to thermoneutral. Cross and Husain [11] have considered the bond energies of various alkyl bromides in some detail [34 - 45] and the conclusions are employed here together with $D^0(n\text{-}C_3H_7Br) = 3.2 \pm 0.3$ eV [46, 47]. Thus, the thermochemistry of the reactions investigated here is estimated as follows:

$$Bi(6^4S^0_{3/2}) + Br_2 \longrightarrow BiBr + Br \qquad \Delta H = -17.8 \pm 0.1 \text{ kcal}$$

$$Bi(6^4S^0_{3/2}) + CH_2Br_2 \longrightarrow BiBr + CH_2Br \qquad \Delta H = 3.8 \pm 5 \text{ kcal}$$

$$Bi(6^4S^0_{3/2}) + CH_3Br \longrightarrow BiBr + CH_3 \qquad \Delta H = 6.8 \pm 1.2 \text{ kcal}$$

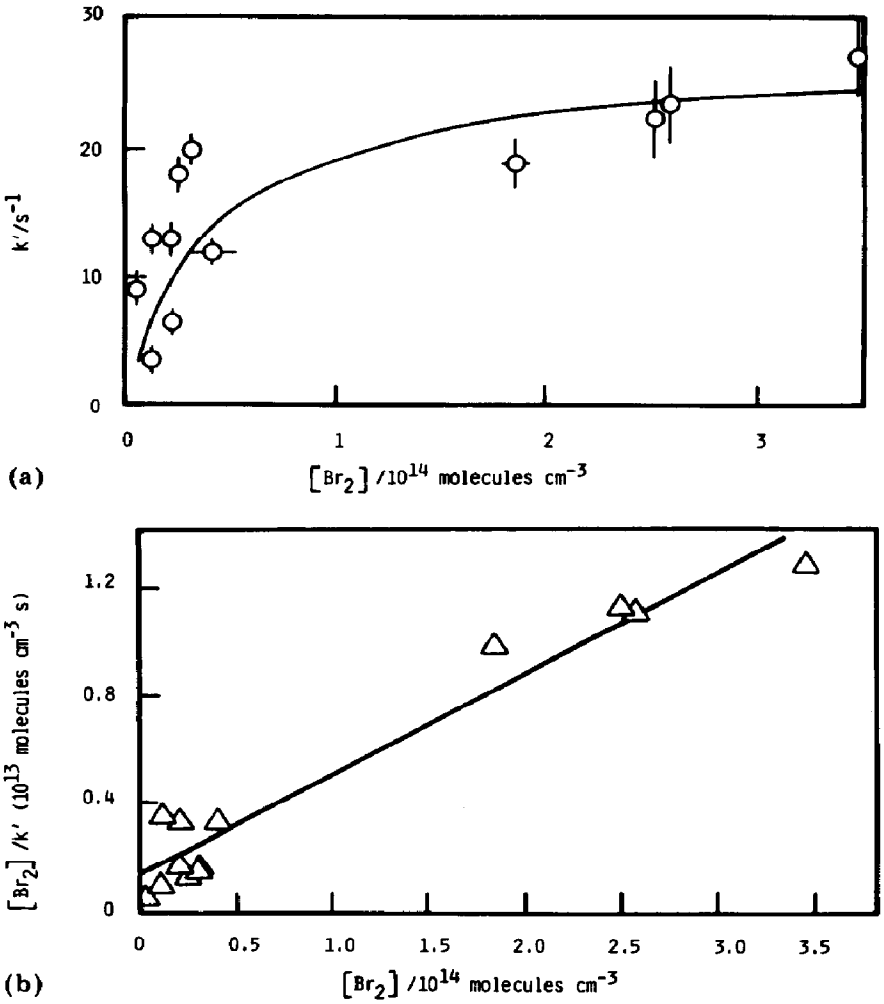

Fig. 9. Variation in the pseudo-first-order rate coefficient k' (diffusion corrected and normalized) for the decay of $Bi(6^4S_{3/2})$ in the presence of Br_2 ($[Bi(CH_3)_3] = 3.1 \times 10^{13}$ molecules cm^{-3}; $[He] = 4.8 \times 10^{17}$ atoms cm^{-3}; $E = 320$ J): (a) k' *vs.* $[Br_2]$; (b) $[Br_2]/k'$ *vs.* $[Br_2]$.

TABLE 1

Absolute second-order constants k_{RBr} (cm^3 molecule^{-1} s^{-1}) ($T = 300$ K; errors, 2σ) for the reaction of $Bi(6^4S^0_{3/2})$ and $Pb(6^3P_0)$ with some bromine-containing molecules

RBr	*Bi*$(6^4S^0_{3/2})$[a]	*Pb*(6^3P_0) [11]
Br_2	$(5.3 \pm 1.8) \times 10^{-13}$	—
CH_3Br	$(1.8 \pm 0.4) \times 10^{-15}$	$(3.7 \pm 1.0) \times 10^{-15}$
C_2H_5Br	$(4.1 \pm 0.7) \times 10^{-15}$	$(5.0 \pm 1.0) \times 10^{-15}$
n-C_3H_7Br	$(1.2 \pm 0.1) \times 10^{-14}$	—
CH_2Br_2	$(9.0 \pm 1.3) \times 10^{-15}$	$(1.4 \pm 0.4) \times 10^{-13}$
CH_3CHBr_2	—	$(6.0 \pm 1.0) \times 10^{-13}$

[a]This work.

$$Bi(6^4S^0_{3/2}) + C_2H_5Br \longrightarrow BiBr + C_2H_5 \qquad \Delta H = 4.6 \pm 2 \text{ kcal}$$

$$Bi(6^4S^0_{3/2}) + n\text{-}C_3H_7Br \longrightarrow BiBr + n\text{-}C_3H_7 \qquad \Delta H = 10.7 \pm 7 \text{ kcal}$$

Simply on the basis of thermochemistry, a major variation in k_{RBr} would not be expected for reactions of $Bi(6^4S^0_{3/2})$ with the alkyl bromides and this is borne out by experiment (Table 1). For CH_3Br and C_2H_5Br, the k_{RBr} values for $Bi(6^4S^0_{3/2})$ and $Pb(6^3P_0)$ are similar in magnitude whereas the reaction of $Pb(6^3P_0)$ with CH_2Br_2 is clearly much more rapid. The relatively rapid reaction rate between $Bi(6^4S^0_{3/2})$ and Br_2 is in accord with both the favourable thermochemistry and the correlations in (J, Ω) coupling $(2E_{1/2})$ [48] connecting ground state reactants and products.

3.3. Radiation trapping

In earlier investigations of time-resolved resonance fluorescence at $\lambda = 306.77$ nm, Husain *et al.* [3] employed the diffusion theory of radiation [12] to deduce the effects of radiation trapping for the $Bi(7^4P_{1/2})$–$Bi(6^4S^0_{3/2})$ transition, restricting calculations to the use of "low equivalent opacities" [49] when applied to the "infinite slab" theory of Milne [50] and the modifications described by Samson [51]. Solutions of the diffusion equations for radiation [52]

$$\nabla^2\left(n^* + \frac{\tau \partial n^*}{\partial t}\right) = \frac{4k^2\tau \partial n^*}{\partial t} \tag{10}$$

were taken from Blickensderfer *et al.* [52] where n^* is the stationary state concentration of $Bi(7^4P_{1/2})$, τ is the natural radiative lifetime and k is the atomic absorption coefficient. This approach employs the approximation that at a single equivalent opacity $\bar{k}R$

$$\exp(-\bar{k}R) = \int_{-\infty}^{\infty} F(\omega) \exp\{-k_0 R F(\omega)\}\, d\omega \Big/ \int_{-\infty}^{\infty} F(\omega)\, d\omega \tag{11}$$

for the spectral distribution of the imprisoned radiation and the line shape $F(\omega)$ of the resonance transition, which may be defined in terms of the Doppler width $\Delta\bar{\nu}_D$ for a Doppler profile or defined in terms of the Doppler width *and* the sum of the dispersion-type widths (in this case, the Lorentz width $\Delta\bar{\nu}_L$ and the Heisenberg width $\Delta\bar{\nu}_N$) for a Voigt profile [12]:

$$\omega = \frac{2(\bar{\nu} - \bar{\nu}_0)}{\Delta\bar{\nu}_D} (\ln 2)^{1/2} \tag{12}$$

$$\alpha = \frac{\Delta\bar{\nu}_N + \Delta\bar{\nu}_L}{\Delta\bar{\nu}_D} (\ln 2)^{1/2} \tag{13}$$

$$k_0 = \frac{9.964 \times 10^{-14}[Bi(6^4S^0_{3/2})]}{\Delta\bar{\nu}_D} \tag{14}$$

In this paper we extend these calculations in a number of ways. Firstly, we explore the effect of radiation trapping to calculate theoretical effective radiative lifetimes and to determine the relationship between fluorescence intensity and $[Bi(6^4S^0_{3/2})]$ as a function of the Voigt profile itself or, alternatively, we may also take account of nuclear hyperfine splitting (NHFS) and employ a line shape for the summation of the Voigt profiles of each NHFS component:

$$F(\omega) = \frac{\alpha}{\pi} \sum_i \int_{-\infty}^{\infty} \frac{N_i \exp(-y^2)\, dy}{\alpha^2 + (\omega_i - y)^2} \tag{15}$$

where $\Sigma N_i = 1$, based on relative intensities (see later). It will be shown that, when NHFS is considered, the parameter α, which reflects the extent of collision broadening, has only a slight effect on the extent of radiation trapping over the range of overall pressures used in this and previous [1] studies.

Secondly, the effects of radiation trapping at "intermediate" densities of $Bi(6^4S^0_{3/2})$, where the Samson–Milne–Blickensderfer model breaks down and where NHFS is not considered, may be further developed in terms of an equivalent opacity based on the theory of Kenty [53 - 56]. Kenty's calculations employ a maxwellian distribution in both the emitting and the absorbing atoms rather than simply using excitation by isotropic monochromatic radiation. Kenty's form of the equivalent opacity may be used to estimate the trapping times at intermediate to high atomic densities by means of Milne's solution [12]:

$$\frac{\tau^*}{\tau} \approx 1 + \left(\frac{2\bar{k}R}{\pi}\right)^2 \tag{16}$$

for an "infinite" slab of width R. (In general, the width of this infinite slab is identified with the radius of an "infinite" cylinder when the boundary conditions are set up for the solution of eqn. (10) [52].)

Finally, the effects of radiation trapping for $Bi(7^4P_{1/2})$–$Bi(6^4S^0_{3/2})$ are calculated according to the solutions of Holstein [57, 58] as modified by Walsh [59] for intermediate to high atomic densities, with and without consideration of NHFS for the boundary conditions of an infinite cylinder of radius R. This approach dispenses with the approximation of the characteristic mean free path of an emitted photon because of the strong frequency dependence of the absorption coefficient of an atomic gas. The optical properties of the system are calculated as a general transport problem by solving a Boltzmann-type integro-differential equation in terms of a transmission coefficient $T(\rho)$ which is the probability of a resonance quantum travelling a distance ρ without being absorbed [57]. This is expressed in the form

$$T(\rho) = \sum_n \int P_n(\bar{\nu}) \exp\left\{\sum_\sigma k_\sigma(\bar{\nu})\rho\right\} d\bar{\nu} \tag{17}$$

over the NHFS components ($\Sigma \int P_n(\bar{\nu})\, d\bar{\nu} = 1$), where ρ is the radius of an infinite cylinder. This transmission coefficient implies a simple form for the trapping time:

$$\frac{\tau^*}{\tau} = \frac{1}{T(R)} \tag{18}$$

Walsh derived a general solution for $1/T(R)$ considering Doppler broadening T_D and collision broadening T_c, using a collision parameter a ($\approx\alpha$ of the Voigt profile (eqn. (13)) and collision–Doppler interference (T_{cD}). These may be applied over the NHFS components (as suggested by Holstein) thus:

$$T_D = \frac{1.6}{k_0 R} \sum_i \frac{1}{\{\pi \ln(N_i k_0 R)\}^{1/2}} \tag{19}$$

$$T_c = \frac{1.115}{\pi^{1/2}} \sum_i \left(\frac{\pi^{1/2} a}{N_i k_0 R} \right)^{1/2} \tag{20}$$

$$T_{cD} = \frac{2a}{\pi} \sum_i \frac{1}{\{\ln(N_i k_0 R)\}^{1/2}} \tag{21}$$

$$\frac{1}{T(R)} = \exp\left(- \frac{\pi T_c^2}{4 T_{cD}^2} \right) \Big/ T_D + \operatorname{erf}\left(\frac{\pi^{1/2} T_c}{2 T_{cD}} \right) \Big/ T_c \tag{22}$$

where $\Sigma N_i = 1$, as before, and $T(R) \to T_D$ as $a \to 0$.

Apart from the fundamental interest in radiation trapping in this system, the results obtained here are applied to the present experimental measurements in two contexts. Firstly, they are related to the functional relationship between the fluorescence intensity I_F and [Bi($6^4S^0_{3/2}$)] and, secondly, the calculated effective radiative lifetime is employed in the Stern–Volmer analysis yielding fluorescence quenching data for Bi($7^4P_{1/2}$).

Figure 10 gives examples of the Voigt profile ($k_\nu/k_0 = F(\omega)$, eqn. (15)) for the resonance transition centred at $\lambda = 306.77$ nm treated as a single atomic line (*i.e.* no NHFS) for two values of α when the Lorentz cross section σ_L^2(Bi—He) = 6.53 Å^2. The Lorentz cross sections were calculated by taking the mean of the atomic or molecular radius of the buffer gas (M ≡ He, N_2 and CF_4) [60] and that of Bi (interpolated from the van der Waal's radii of group V atoms) [61]. This calculation probably underestimates the true cross sections [12]. Integrals for the Voigt profile were computed according to the appropriate fast subroutine of Sundius [62], and the overall integrals for the equivalent opacity given both by Kenty and by Samson and Milne were solved numerically by the Gaussian–Quadrature method described by Patterson [63]. Figure 11 shows the Voigt profile where the NHFS data were taken from the high resolution optical spectroscopic measurements of Magnante and Stroke [64] who also calculated the relative intensities for

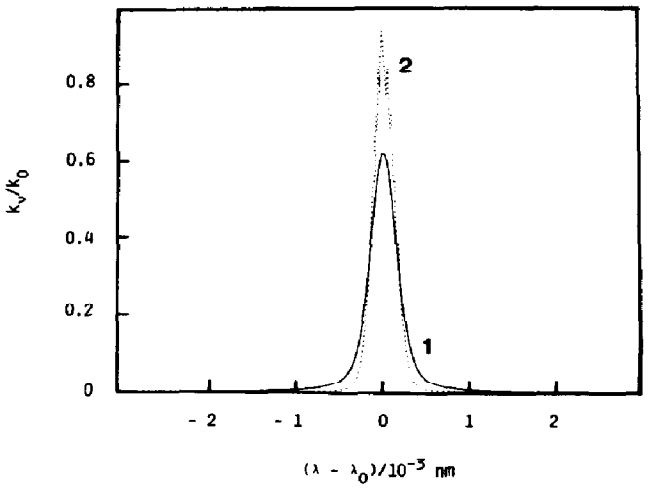

Fig. 10. Example of the computerized simulation of the Voigt profile for a single line atomic transition excluding NHFS for $Bi(7^4P_{1/2}) \rightarrow Bi(6^4S_{3/2})$ at $\lambda = 306.77$ nm (τ_e = 5.9 ns; T = 298 K; k_ν/k_0 *vs.* λ (nm)): curve 1, $\alpha = 0.5$ ($p_{He} \approx 25$ kN m^{-2}); curve 2, α = 0.1165 ($p_{He} \approx 4.7$ kN m^{-2}).

each NHFS component. This profile can be compared with the earlier line shape by Husain *et al.* [3] where a smoother function was the result of amplification of the Lorentz width (larger α). The value for α in Fig. 11 is closer to the experimental conditions, however, on the assumption that the above-stated Lorentz cross section is correct. Furthermore, the present line shape (and all subsequent calculations using $F(\omega)$ and k_0) use the more recent radiative lifetime reported by Cunningham and Link [13] of 5.9 ns compared with the earlier value of 0.71 ns following Corliss and Bozmann [65].

Figure 12 shows the effect on the trapping times τ^*/τ of increasing opacity (R is the radius of an "infinite" cylinder or width of an "infinite" slab).

(1) Without considering NHFS, τ^*/τ is increased by at least one order of magnitude for $[Bi(6^4S^0_{3/2})] \times R > 10^{12}$ atoms cm^{-2}.

(2) Where the Holstein–Walsh and the Samson–Milne–Blickensderfer curves intersect indicates the change from "low" to "intermediate" opacities.

(3) Given that the Holstein–Walsh calculations are easier to perform than those of Kenty (which assume small collisional broadening of a single atomic line, in any case), the Holstein–Walsh approach is far preferable for intermediate to high opacities ($[Bi(6^4S^0_{3/2})] \times R > 5 \times 10^{13}$ atoms cm^{-2}).

The kinetic measurements on $Bi(6^4S^0_{3/2})$ of the type presented in Fig. 3, analysed by means of eqns. (5) and (6), depend on effective linearity of I_F on $Bi(6^4S^0_{3/2})$. For the ideal axial model, the intensity of fluorescence is directly proportional to the incident (continuum) intensity from the resonance source and the total absorption factor:

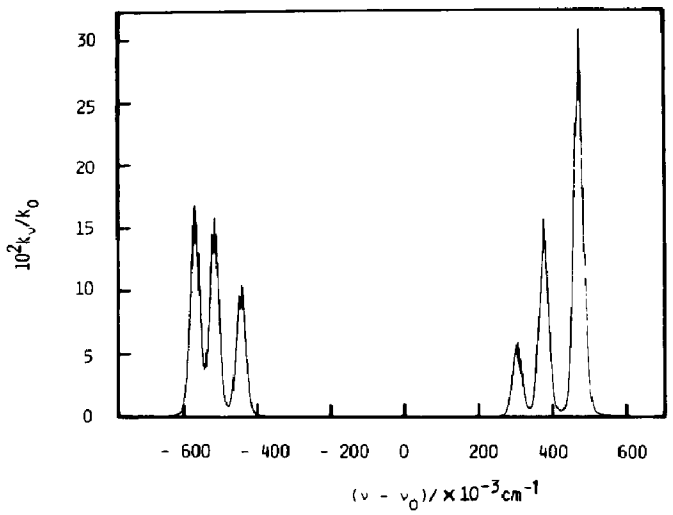

Fig. 11. Example of the computer simulation of the atomic transition at $\lambda = 306.77$ nm ($Bi(7^4P_{1/2}) \rightarrow Bi(6^4S_{3/2})$) indicating the summation of the Voigt profiles over the transitions associated with the individual nuclear hyperfine components ($\tau_e = 5.9$ ns; $T = 298$ K; $\alpha = 0.1171$; $p_{He} \approx 4.75$ kN m^{-2}) (hyperfine interaction constant for $Bi(7^4P_{1/2})$, $A = 164.18 \times 10^{-3}$ cm^{-1}; hyperfine interaction constants for $Bi(6^4S_{3/2})$, $A = -14.909 \times 10^{-3}$ cm^{-1}, $B = -10.149 \times 10^{-3}$ cm^{-1}). The components were measured from a line centre taken as exactly $\lambda = 306.77$ nm.

Position ($\times 10^{-3}$ cm^{-1})	*Relative intensity*
−570	0.175
−517	0.165
−444	0.110
304	0.061
376	0.165
472	0.324

$$I_F \propto I_\omega \int_{-\infty}^{\infty} [1 - \exp\{-k_0 l F(\omega)\}] \, d\omega \tag{23}$$

where the symbols retain their previous meaning. Figure 13(a) shows the result of such a calculation for the same experimental conditions as in Figs. 10 - 12, and l is the unit path length (designated R in the diagram) and is the *diameter* of the infinite cylinder for calculations of trapping times. (It should be noted that when plotted on a *linear* scale along the x axis, the curvature of I_F is *downwards*.) More realistic to the present experimental situation, however, is to consider *reabsorption* of the fluorescence signal as it travels radially from the axis of the resonance source [66]:

$$I_F = \left\{ (\text{constant} \times l'') \Big/ k_0 \int_{-\infty}^{\infty} F(\omega') \, d\omega' \right\} \int_{-\infty}^{\infty} I_\omega [1 - \exp\{-k_0 l F(\omega)\}] \, d\omega \times$$
$$\times \int_{-\infty}^{\infty} [1 - \exp\{-k_0 l' F(\omega')\}] \, d\omega' \tag{24}$$

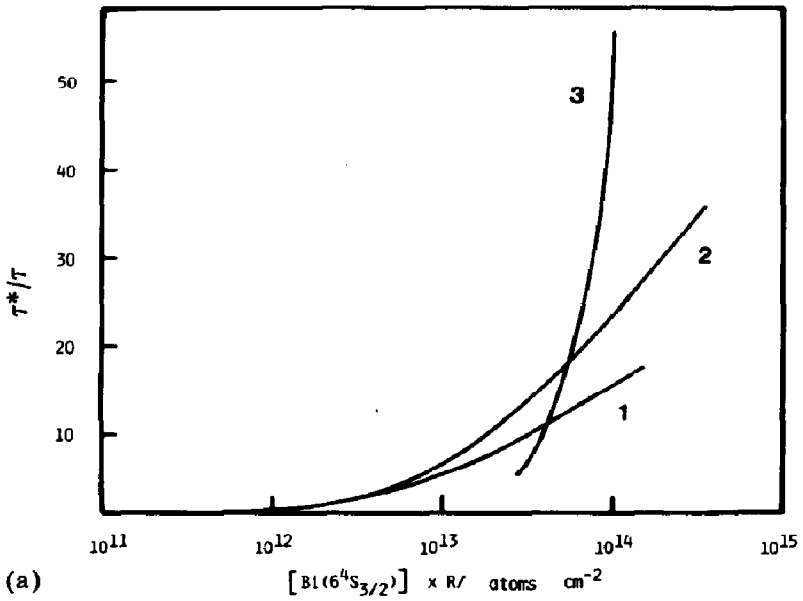

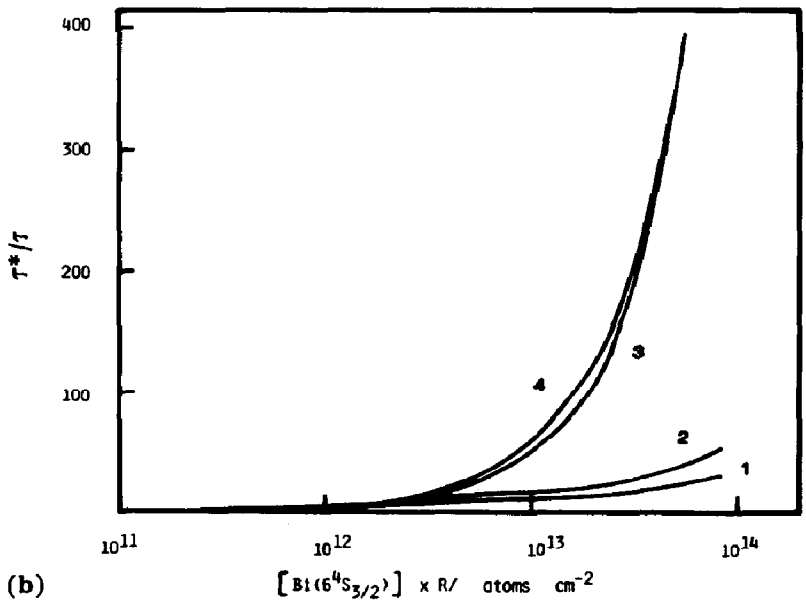

Fig. 12. Plots of apparent relative radiative lifetimes for the transition Bi($7^4P_{1/2}$) → Bi($6^4S_{3/2}$) (λ = 306.77 nm) as a function of ground state atomic bismuth concentration for radiation trapping calculations (a) including NHFS (curve 1, Samson–Milne–Blickensderfer (infinite slab geometry); curve 2, Samson–Milne–Blickensderfer (cylindrical geometry); curve 3, Holstein–Walsh (cylindrical geometry)) and (b) without NHFS (R, unit path length) (curve 1, Samson–Milne–Blickensderfer (infinite slab geometry); curve 2, Samson–Milne–Blickensderfer (cylindrical geometry); curve 3, Holstein–Walsh; curve 4, Kenty).

where, for our unit cell, $l = l' = l''$, $\omega = \omega'$ and I_ω = constant. For a continuum source

$$I_F \propto \frac{1}{k_0 l}\left(\int_{-\infty}^{\infty} [1 - \exp\{-k_0 l F(\omega)\}]\, d\omega\right)^2 \qquad (25)$$

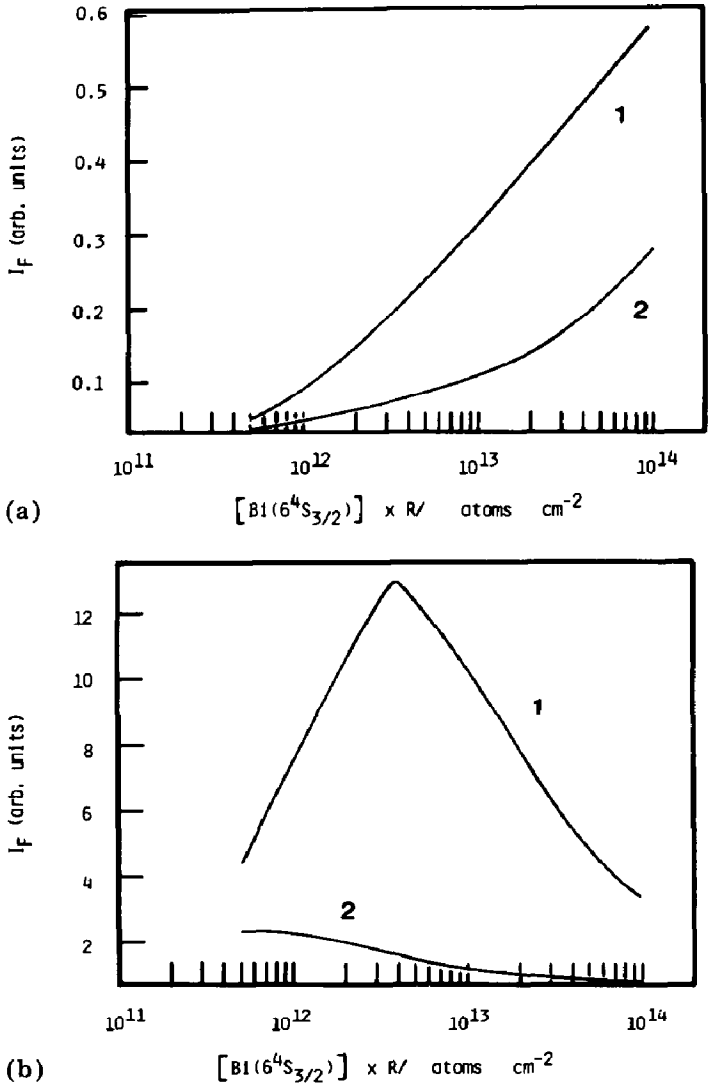

Fig. 13. Variation in the fluorescence intensity I_F of $Bi(7^4P_{1/2}) \rightarrow Bi(6^4S_{3/2})$ (λ = 306.77 nm) with ground state atomic bismuth concentration for (a) axial observation and (b) radial observation (R, unit path length): curve 1, including NHFS; curve 2, without NHFS.

and again l is twice the radius of an infinite cell (but designated R in Fig. 13(b)) and $k_0 \propto [Bi(6^4S^0_{3/2})]$. Hence, it is possible to calibrate $[Bi(6^4S^0_{3/2})] \times l$ of this unit cell against the density of the photochemical precursor, $Bi(CH_3)_3$, under the appropriate experimental conditions, and thence to deduce the opacity for the trapping time calculations (Fig. 12, $[Bi(6^4S^0_{3/2})] \times l = 2[Bi(6^4S^0_{3/2})] \times R$). This is shown in Figs. 14 and 15. This calculation implies a production of $Bi(6^4S^0_{3/2})$ from $Bi(CH_3)_3$ of only 1%; however, l may be less than unity, and the production of ground state bismuth atoms from $Bi(CH_3)_3$ is presumably a multiquantum process so that even though the

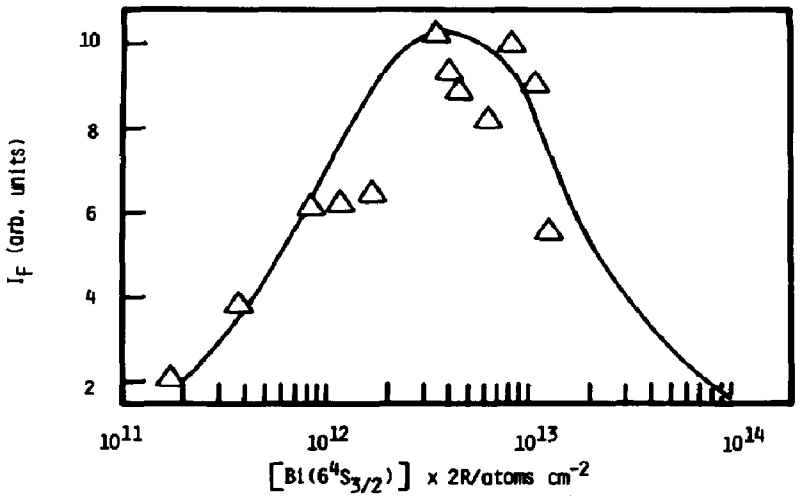

Fig. 14. Comparison of the relationship between the fluorescence intensity I_F at λ = 306.77 nm ($Bi(7^4P_{1/2})$–$Bi(6^4S_{3/2})$) and the atomic density of $Bi(6^4S_{3/2})$ (R, unit path length): ——, calculated for radiation trapping including NHFS with radial observation; △, data points from time-resolved atomic resonance fluorescence measurements (via θ_2) on $Bi(6^4S_{3/2})$ in the presence of N_2, corrected for fluorescence quenching.

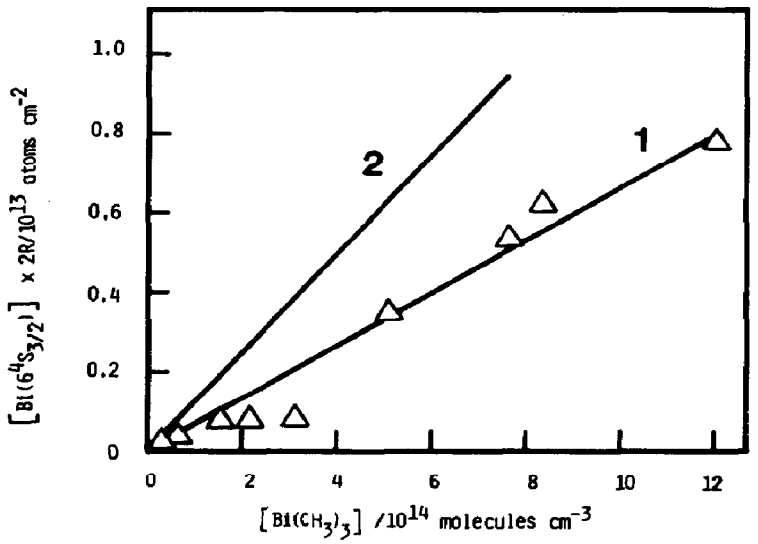

Fig. 15. Comparison of the relationship between $[Bi(6^4S_{3/2})] \times 2R$ (R, unit path length) derived from radiation trapping calculations including NHFS for radial observation and $[Bi(CH_3)_3]$ resulting from the relationship between I_F and $Bi(CH_3)_3$: curve 1, flash photolysis lamp following ref. 1; △, data points using N_2 as added gas; curve 2, calculation for present flash photolysis lamp.

photolysis of $Bi(CH_3)_3$ may be complete (see Section 3.1) the photofragments could exist largely in the form of $BiCH_3$ and $Bi(CH_3)_2$. One further comment is necessary concerning the uncertain value of the Lorentz cross sections (and therefore α, eqn. (13)) used in the radiation trapping calculations. Calculations show that although curves of I_F *versus* $[Bi(6^4S^0_{3/2})] \times l$

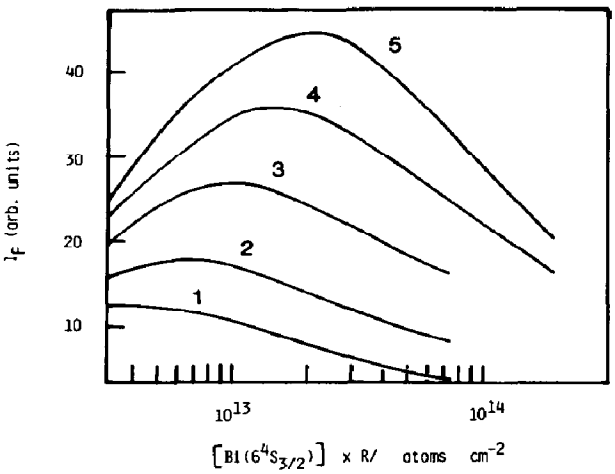

Fig. 16. Variation in the fluorescence intensity I_F of Bi($7^4P_{1/2}$) → Bi($6^4S_{3/2}$) (λ = 306.77 nm) with ground state atomic bismuth concentration for radial observation with different Voigt profiles including NHFS: curve 1, α = 0.1; curve 2, α = 0.5; curve 3, α = 1.5; curve 4, α = 3; curve 5, α = 5.

(Fig. 16) become steeper with increasing α ($\Delta\bar{\nu}_D$ fixed), the values of X = [Bi($6^4S^0_{3/2}$)] × l corresponding to $I_F{}^{max}$ are not shifted greatly: $X(I_F{}^{max})((\alpha = 0.1):(\alpha = 0.5):(\alpha = 1.5)) = 1:1.75:2.75$. Also, at fixed [Bi($6^4S^0_{3/2}$)] × R (5×10^{12} atoms cm^{-2}), $\tau^*/\tau((\alpha = 0.1):(\alpha = 0.5):(\alpha = 1.5)) = 1:0.8:0.5$. For the present type of measurements realistic values of α lie in the range $0 < \alpha < 0.75$.

3.4. Fluorescence quenching of Bi($7^4P_{1/2}$)

We have shown that the combination of eqns. (5) and (6) can be used to determine fluorescence quenching data for Bi($7^4P_{1/2}$) [1]. Thus, for a single quenching species Q the ratio of the slope to the intercept of a plot of $1/\theta_2$ *versus* [Q] (Stern–Volmer plot) yields k_Q/gk_f. Alternatively, for a mixture of gases with [Q_1] (fixed) and [Q_2] (varied), the ratio of the slope to the intercept of the plot of $1/\theta_2$ *versus* [Q_2] is given by $k_{Q_2}/(k_{Q_1}[Q_1] + gk_f)$. In most cases, the excess helium buffer gas is the only further species (Q_1) present in any significant quantity and is characterized by a negligible quenching rate constant. We have also stressed that the error in θ_2 is inherently larger than that for k' because of fluctuations in output of both the flash-lamp and the resonance source.

Data for k_Q that we have reported previously [1] have been adjusted to allow for radiation trapping as indicated. The cross sections are calculated according to $k_Q = (8\pi RT/\mu)^{1/2}\sigma^2$. Table 2 presents the corrected cross sections (error, about 30%) and the estimated trapping times ($\tau^*/\tau = 1/g$, eqn. (5)). In comparison with the cross sections reported by Connor *et al.* [9, 13] our value for $\sigma^2(O_2)$ is high, even when Connor's limits (for experimental error and possible radiation trapping) are considered: $0.08 < \sigma^2$ (Å^2) < 143 compared with our limits of $400 < \sigma^2$ (Å^2) < 676. The effect of

TABLE 2

Quenching cross sections, experimental conditions and calculated ratios of lifetimes with radiation trapping (τ^*) and without radiation trapping (τ = 5.9 ns) for quenching of $Bi(7^4P_{1/2})$ by gas Q (λ = 306.77 nm; $Bi(7^4P_{1/2})$–$Bi(6^4S^0_{3/2})$; T = 298 K; $\Delta\bar{\nu}_D = 27.9 \times 10^{-3}$ cm^{-1}; $\Delta\bar{\nu}_N = 0.9 \times 10^{-3}$ cm^{-1})

Q	$[Bi(6^4S^0_{3/2}) \times 2R]$ ($\times 10^{11}$ atoms cm^{-2})	$\Delta\bar{\nu}_L$ ($\times 10^{-3}$ cm^{-1})	τ^*/τ [a]	σ^2 ($\times 10^{-16}$ cm^2 molecule^{-1})
N_2	14[b]	3.02	1.33	2.9[c]
O_2	3.1[b]	1.79	1.09	520[c]
C_2H_2	18[b]	2.74	1.43	69[c]
N_2O	24[b]	2.51	1.60	110[c]
NO	16[b]	4.84	1.35	126[c]
CF_4	15[b]	2.08	1.41	11[c]
CH_3Br	4.5[d]	1.27	1.12	< 590[e]
C_2H_5Br	6.0[d]	4.95	1.13	< 370[e]
n-C_3H_7Br	1.4[d]	0.83	1.04	< 140[e]

[a] Cylindrical geometry.
[b] See Fig. 15, curve 1.
[c] Corrected data from ref. 1.
[d] See Fig. 15, curve 2.
[e] This work (upper limits, see text).

even slight depletion of the precursor, $Bi(CH_3)_3$, before photolysis and, in the case where Q ≡ RBr, screening by RBr of the actinic radiation will significantly affect any Stern–Volmer plot leading to systematic overestimation of k_Q; this was found to be particularly true in the cases of Q ≡ Br_2 and CH_2Br_2 which are omitted from the data presented (Table 2). Thus although the Stern–Volmer plots for the present work (Fig. 17) demonstrate a varia-

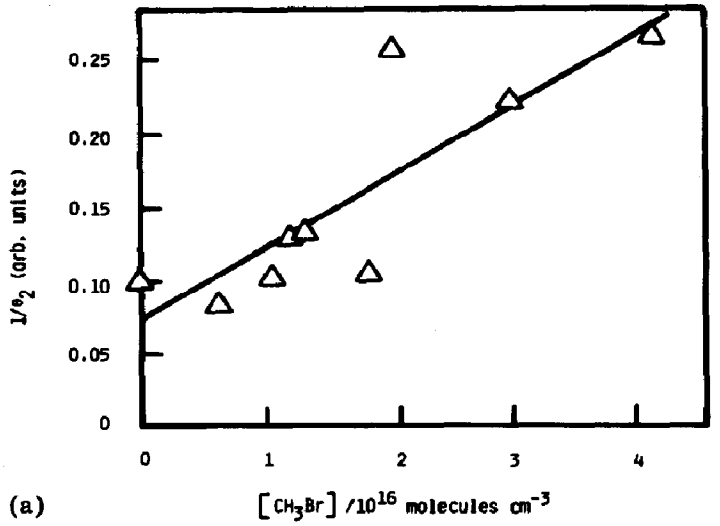

(a)

Fig. 17 *(continued)*.

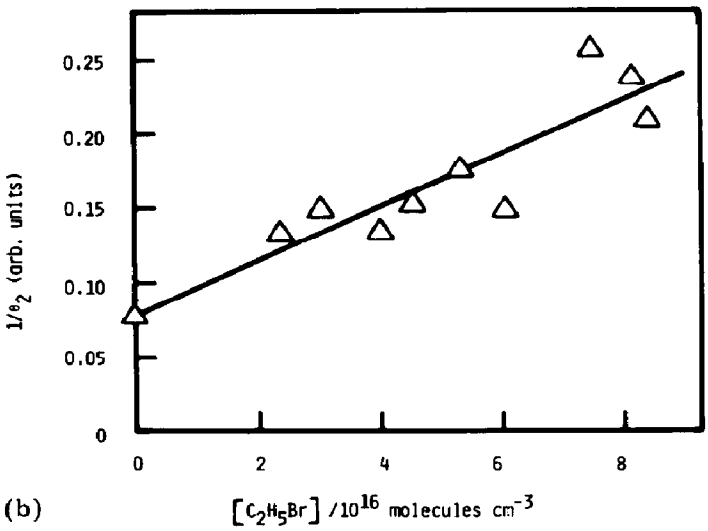

Fig. 17. Stern–Volmer plots ($1/\theta_2$ *vs.* [Q]) for the collisional quenching of $Bi(7\,^4P_{1/2})$ by (a) CH_3Br and (b) C_2H_5Br obtained by time-resolved atomic resonance fluorescence at λ = 306.8 nm ($7\,^4P_{1/2}$–$6\,^4S_{3/2}$) following the flash photolysis of $Bi(CH_3)_3$ (E = 320 J): (a) CH_3Br ($[Bi(CH_3)_3] = 3.6 \times 10^{13}$ molecules cm^{-3}; $[He] = 4.8 \times 10^{17}$ atoms cm^{-3}); (b) C_2H_5Br ($[Bi(CH_3)_3] = 4.8 \times 10^{13}$ molecules cm^{-3}; $[He] = 18.7 \times 10^{17}$ atoms cm^{-3}).

tion in θ_2 (which is a function of $k_Q[Q]$ *and* $[Bi(6\,^4S^0_{3/2})]_{t=0}$) similar to those hitherto [1] for gases sensibly unaffected by screening, the cross sections presented for RBr in Table 2 must be regarded as upper limits.

References

1 C. F. Bell and D. Husain, *J. Photochem., 24* (1984) 207.
2 C. F. Bell and D. Husain, *J. Photochem., 24* (1984) 223.
3 D. Husain, L. Krause and N. K. H. Slater, *J. Chem. Soc., Faraday Trans. II, 73* (1977) 1678.
4 D. Husain, L. Krause and N. K. H. Slater, *J. Chem. Soc., Faraday Trans. II, 73* (1977) 1706.
5 D. Husain and N. K. H. Slater, *J. Chem. Soc., Faraday Trans. II, 73* (1978) 1222.
6 D. Husain and N. K. H. Slater, *J. Chem. Soc., Faraday Trans. II, 73* (1978) 1627.
7 J. H. Lee, J. V. Michael, W. A. Payne and L. J. Stief, *J. Chem. Phys., 69* (1978) 3069.
8 D. Husain and N. K. H. Slater, *J. Chem. Soc., Faraday Trans. II, 76* (1980) 606.
9 J. Connor, P. J. Young and O. P. Strausz, *J. Am. Chem. Soc., 93* (1971) 822.
10 D. Husain and N. K. H. Slater, *J. Photochem., 6* (1977) 325.
11 P. J. Cross and D. Husain, *J. Photochem., 8* (1978) 183.
12 A. C. G. Mitchell and M. W. Zemansky, *Resonance Radiation and Excited Atoms*, Cambridge University Press, Cambridge, Cambs., 1971.
13 P. T. Cunningham and J. K. Link, *J. Opt. Soc. Am., 57* (1967) 1000.
14 C. I. M. Beenakker, *Spectrochim. Acta, Part B, 31* (1976) 483.
15 C. I. M. Beenakker, *Spectrochim. Acta, Part B, 32* (1977) 173.
16 C. I. M. Beenakker and P. W. J. M. Boumans, *Spectrochim. Acta, Part B, 33* (1978) 53.
17 W. H. Wing and T. M. Sanders, Jr., *Rev. Sci. Instrum., 36* (1965) 294.
18 M. I. Christie and G. Porter, *Proc. R. Soc. London, Ser. A, 212* (1952) 398.

19 J. D. Smith, in J. C. Bailar, H. J. Emeleus, R. Nyholm and A. F. Trotman-Dickenson (eds.), *Comprehensive Inorganic Chemistry*, Vol. 2, Pergamon, Oxford, 1973, p. 624.
20 D. Husain and N. K. H. Slater, *J. Photochem.*, *7* (1977) 59.
21 D. Porret and C. F. Goodeve, *Proc. R. Soc. London, Ser. A*, *165* (1938) 31.
22 J. G. Calvert and J. N. Pitts, Jr., *Photochemistry*, Wiley, New York, 1966.
23 R. J. Donovan and D. Husain, *Trans. Faraday Soc.*, *62* (1962) 2643.
24 C. Ting and R. E. Weston, Jr., *J. Phys. Chem.*, *77* (1973) 2257.
25 H. Okabe, *Photochemistry of Small Molecules*, Wiley, New York, 1978, p. 300.
26 M. J. D. Powell, personal communication, 1979, cited in D. Husain and N. K. H. Slater, *J. Chem. Soc., Faraday Trans. II*, *76* (1980) 606.
27 M. W. Zemansky, *Phys. Rev.*, *34* (1929) 213.
28 A. G. Gaydon, *Dissociation Energies and Spectra of Diatomic Molecules*, Chapman and Hall, London, 1968.
29 S. Sankaranarayan, M. M. Patel and P. S. Narayanan, *Proc. Indian Acad. Sci., Sect. A*, *56* (1962) 171.
30 S. P. Singh, *Indian J. Pure Appl. Phys.*, *6* (1968) 299.
31 K. P. Huber and G. Herzberg, *Molecular Spectra and Molecular Structure*, Vol. IV, *Constants of Diatomic Molecules*, Van Nostrand Reinhold, New York, 1979.
32 K. Wieland and R. Newburgh, *Helv. Phys. Acta*, *25* (1952) 87.
33 R. F. Barrow, in B. Rosen (ed.), *Spectroscopic Data Relative to Diatomic Molecules*, Pergamon, Oxford, 1970.
34 F. P. Losing, K. U. Ingold and I. H. S. Henderson, *J. Chem. Phys.*, *22* (1954) 1489.
35 M. Szwarc, *Chem. Rev.*, *47* (1950) 75.
36 M. Szwarc, *Q. Rev., Chem. Soc.*, *5* (1951) 22.
37 A. R. Irsa, *J. Chem. Phys.*, *26* (1957) 18.
38 C. T. Mortimer, *Reaction Heats and Bond Strengths*, Pergamon, Oxford, 1962.
39 T. L. Cottrell, *Strengths of Chemical Bonds*, Butterworths, London, 1961.
40 G. Herzberg, *Molecular Spectra and Molecular Structure*, Vol. III, *Electronic Structure of Polyatomic Molecules*, Van Nostrand Reinhold, New York, 1966.
41 J. A. Kerr and A. F. Trotman-Dickenson, in R. C. Weast (ed.), *Handbook of Chemistry and Physics*, CRC Press, Cleveland, OH, 57th edn., 1976.
42 S. W. Benson, *Thermochemical Kinetics*, Wiley, New York, 1969.
43 K. C. Ferguson, E. N. Okafo and E. Whittle, *J. Chem. Soc., Faraday Trans. I*, *69* (1973) 295.
44 J. D. Cox and G. Pilcher, *Thermochemistry of Organic and Organometallic Compounds*, Academic Press, New York, 1972.
45 V. I. Vedeneyev, L. V. Gurvich, V. N. Kondratiev, V. A. Medvedev and Y. L. Frankevich, *Bond Energies, Ionization Potentials and Electron Affinities*, Akademia Nauk, Moscow, 1974.
46 S. Tsuda and W. H. Hamill, *J. Chem. Phys.*, *41* (1964) 2713.
47 J. D. Franklin, J. G. Dillard, H. M. Rosenstock, J. T. Herron and K. Draxel, Ionization potentials, appearance potentials and heats of formation of gaseous positive ions, *Rep. NSRDS-NBS-26*, 1969 (National Bureau of Standards, U.S. Department of Commerce, Washington, DC).
48 D. Husain, *Ber. Bunsenges. Phys. Chem.*, *81* (1977) 168.
49 J. V. Michael and C. Yeh, *J. Chem. Phys.*, *53* (1970) 59.
50 E. A. Milne, *J. London Math. Soc.*, *1* (1926) 40.
51 E. W. Samson, *Phys. Rev.*, *40* (1932) 940.
52 R. P. Blickensderfer, W. H. Breckenridge and J. Simons, *J. Chem. Phys.*, *80* (1976) 653.
53 C. Kenty, *Phys. Rev.*, *31* (1928) 997.
54 C. Kenty, *Phys. Rev.*, *42* (1932) 823.
55 M. W. Zemansky, *Phys. Rev.*, *29* (1927) 513.
56 M. W. Zemansky, *Phys. Rev.*, *42* (1932) 843.
57 T. Holstein, *Phys. Rev.*, *72* (1947) 1212.

58 T. Holstein, *Phys. Rev.*, *83* (1951) 1159.
59 P. J. Walsh, *Phys. Rev.*, *116* (1959) 511.
60 J. O. Hirschfelder, C. F. Curtiss and R. B. Bird, *Molecular Theory of Gases and Liquids*, Wiley, New York, 1964.
61 R. C. Weast (ed.), *Handbook of Physics and Chemistry*, CRC Press, Cleveland, OH, 55th edn., 1975.
62 T. Sundius, *J. Raman Spectrosc.*, *1* (1973) 471.
63 T. N. L. Patterson, NAG.FORTLIB, Mk 10, D01ARF and D01AHF, *Math. Comput.*, *22* (1968) 847.
64 P. C. Magnante and H. H. Stroke, *J. Opt. Soc. Am.*, *59* (1969) 836.
65 C. H. Corliss and W. R. Bozmann, *Experimental Transition Probabilities for Spectral Lines of Seventy Elements, Natl. Bur. Stand. (U.S.), Monogr.*, *53* (1962).
66 G. F. Kirkbright and M. Sargent, *Atomic Absorption and Fluorescence Spectroscopy*, Academic Press, London, 1974, pp. 78 ff.